Supramolecular formation of fibrous nanostructure in donor–acceptor dyad film†

Takeshi Nishizawa, Keisuke Tajima* and Kazuhito Hashimoto*

Received 30th January 2007, Accepted 19th March 2007
First published as an Advance Article on the web 3rd April 2007
DOI: 10.1039/b701438d

A novel oligothiophene and its fullerene derivative were synthesized and their film morphologies were investigated. AFM images revealed that the oligothiophene formed well-aligned fiber-like nanostructures in the film after being thermally annealed at its liquid-crystalline temperature. In the oligothiophene–fullerene dyad film, fibers were already formed in the as-cast film. Thermal annealing further enhanced the structural order and a long, partially aligned fibrous nanostructure with a width of around 10 nm and a length of as long as 200 nm was observed. Combined with the results of X-ray analysis, these features were ascribed to supramolecular self-assembly *via* π–π interaction of the oligothiophene groups. Photovoltaic properties of the molecules were also investigated.

Introduction

Nanostructure formation in organic thin solid films is of high importance in intermolecular opto-electronic processes such as photo-induced energy and electron transfer. Self-assembly of organic molecules is one of the powerful tools used to control such nanostructures and to fine-tune the electronic interactions between the molecules.[1,2] π-Conjugated oligomers, often combined with hydrogen-bonding moieties, have been known to achieve such supramolecular organization through their strong π–π interaction.[1–12] 1-D structures of the π-conjugated oligomers have been successfully formed in the films, resulting in efficient charge transport or energy transfer.[3–6]

Moreover, supramolecular organization of donor–acceptor (D–A) multifunctional molecules is of great interest to achieve efficient photo-induced charge separation and subsequent transport of both holes and electrons in the film. However, only a limited number of studies have been done on supramolecular nanostructures of the D–A molecules in the solid state,[7,13] compared to examples of their self-assembly in solution.[14–20]

Herein, we report the syntheses of a novel oligothiophene and its fullerene derivative (**1** and **2** in Fig. 1, respectively). The oligothiophene and the fullerene groups in the dyad **2** were introduced as a donor and an acceptor, respectively. It was also designed that the fullerene group works as another driving force to form a supramolecular self-assembly *via* its strong self-aggregation tendency in addition to the π–π interaction of the oligothiophene group. The long, flexible oligo(ethyleneoxide) spacer connected the lateral position of the oligothiophene group to the fullerene group, to effectively separate each group and thus to enhance their own interactions. As a result, fiber-like nanostructures were successfully fabricated by self-assembly of the molecules in the films. Their photo-physical and photovoltaic properties were also investigated.

Department of Applied Chemistry, Graduate School of Engineering, The University of Tokyo, 7-3-1 Hongo, Bunkyo-ku, Tokyo, 113-8656, Japan. E-mail: k-tajima@light.t.u-tokyo.ac.jp; hashimoto@light.t.u-tokyo.ac.jp; Fax: +81-3-5841-8751; Tel: +81-3-5841-7244

† Electronic supplementary information (ESI) available: detailed synthetic schemes, NMR and MS spectra of **1** and **2**, DSC chart of **2**. See DOI: 10.1039/b701438d

Results and discussion

Synthesis†

The oligothiophene **1** was synthesized *via* a Pd^0-catalyzed Stille cross-coupling reaction, followed by cleavage of tetrahydropyranyl ether (THP) (Scheme 1). The 2,5-bis-stannylthiophene derivative **4** and 2 equivalents of the terthiophene derivative with long alkyl chains **5** were employed in the coupling reaction. The toluene solution of the mixture of **4** and **5** with 5 mol% of $Pd^0(PPh_3)_4$ was refluxed overnight, resulting in the oligothiophene derivative with a THP group (**6** in Scheme 1). The product **6** and pyridinium *p*-toluenesulfonate were dissolved in $CHCl_3$–EtOH. The mixture solution was stirred at 60 °C for 19 h, yielding oligothiophene **1**. The dyad **2** was synthesized *via* subsequent esterification reaction with the fullerene derivative bearing a carboxylic chloride group **7** (Scheme 2). The products were characterized by ^{1}H-NMR and MALDI TOF-MS.†

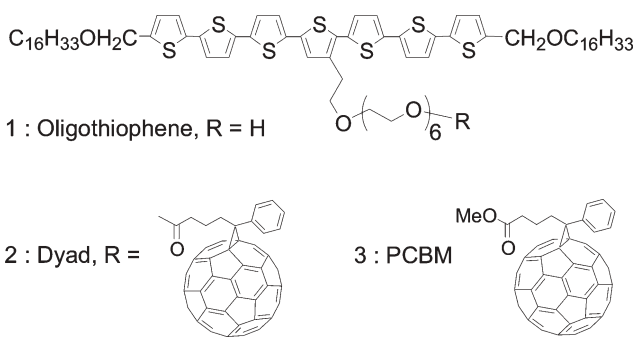

Fig. 1 Molecular structures of oligothiophene **1**, dyad **2**, and PCBM **3**.

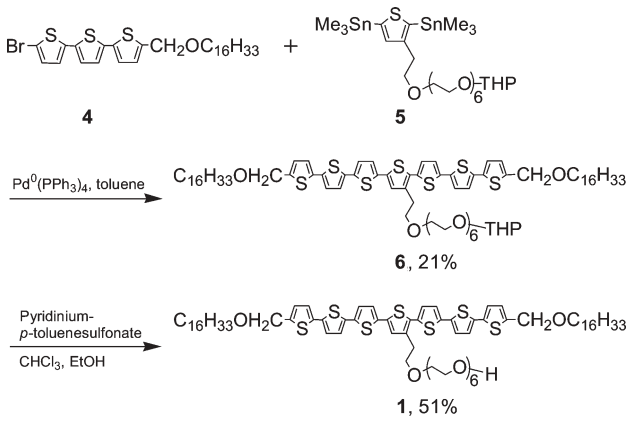

Scheme 1 Synthesis of oligothiophene **1**.

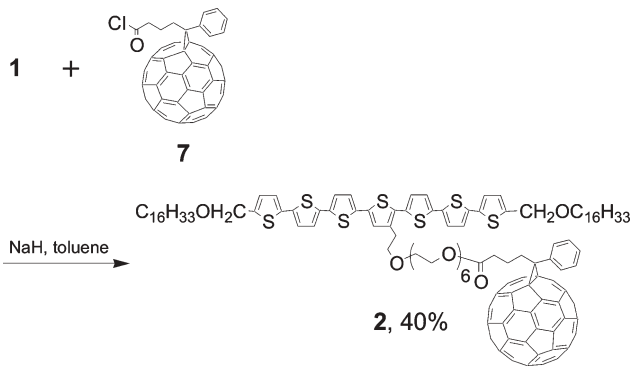

Scheme 2 Synthesis of dyad **2**.

Thermal behavior

The thermal behavior of the oligothiophene **1** and the dyad **2** was investigated by differential scanning calorimetry (DSC) and polarized optical microscopy (POM). Fig. 2 shows the DSC chart of the oligothiophene **1** at a scan rate of 10 °C min^{-1}. Upon heating, two endothermic peaks were observed at 73 °C and 105 °C. POM observation reveals that at 73 °C the crystalline phase turned into the liquid-crystalline phase, and at 105 °C to the isotropic phase. The POM picture

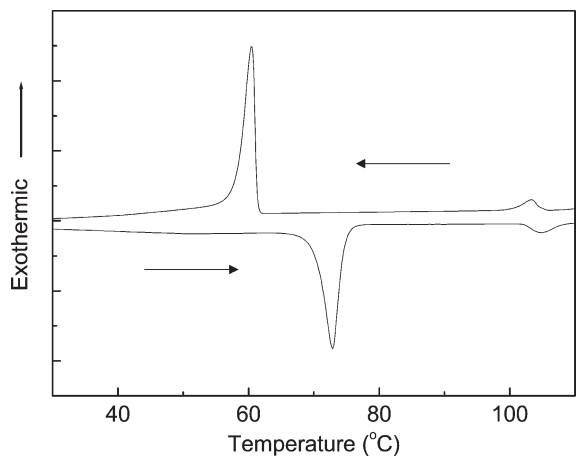

Fig. 2 DSC Chart of the oligothiophene **1**, obtained at a scan rate of 10 °C min^{-1}.

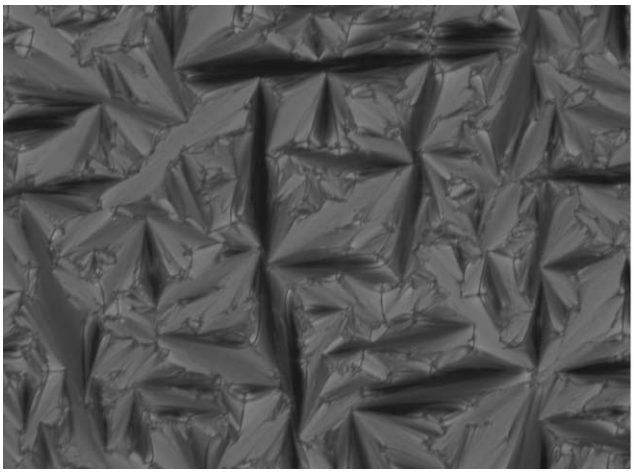

Fig. 3 Polarized optical microscope picture of the liquid-crystalline texture of the oligothiophene **1** at 100 °C taken during the cooling process.

of the liquid-crystalline phase of **1** (Fig. 3) shows a focal-conic fan texture. An XRD pattern at around 80 °C (Fig. 4) shows a diffraction peak at 48.5 Å and the secondary order diffraction peak at 24.7 Å, which could correspond to the layer distance of the oligothiophenes with the alkyl side-chains interdigitated. From the POM and XRD results, the liquid-crystalline phase of **1** can be assigned to a smectic A phase.

In contrast to liquid-crystal formation of the oligothiophene **1**, the dyad **2** did not show any liquid-crystalline phases but simply melted at 52 °C. The bulkiness and/or the strong aggregation tendency of the fullerene groups might weaken the π–π interaction of the oligothiophene groups, resulting in disturbing the liquid-crystal formation.

Surface morphology

Surface morphology of the thin films of the oligothiophene **1** and the dyad **2** were investigated by atomic force microscopy (AFM). Thin films of **1** and **2** were prepared by spin-coating on indium tin oxide (ITO)-coated glass/poly(3,4-ethylenedioxythiophene)–poly(styrenesulfonic acid) (PEDOT–PSS) substrates from $CHCl_3$ solution. AFM phase images of the oligothiophene **1** showed bundles of fibers aggregated in a

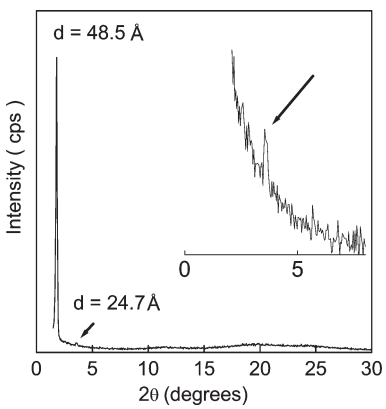

Fig. 4 The XRD pattern of the liquid-crystalline phase of the oligothiophene **1**, measured during the cooling process (82.6–79.2 °C).

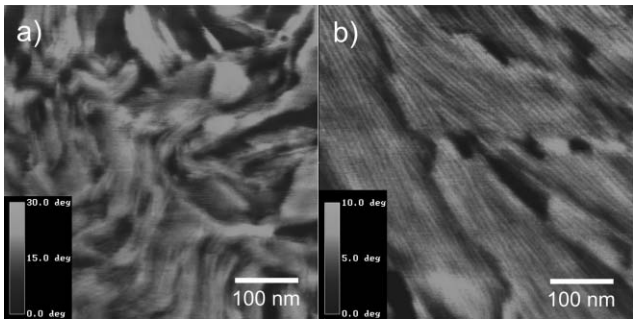

Fig. 5 AFM phase images of the oligothiophene **1** in a) as-coated and b) thermally annealed (at 80 °C for 5 min) films on ITO/PEDOT–PSS substrates.

random orientation (Fig. 5a). To enhance molecular alignment in the film, thermal annealing was conducted at a liquid-crystalline temperature (80 °C) for 5 minutes under N_2. As a result, the molecular alignment was expectedly enhanced and oligothiophene **1** formed fiber-like nanostructures in the film (Fig. 5b). This kind of feature has been reported in several liquid-crystalline molecules.[21] Thus, we attributed the molecular alignment in the oligothiophene film observed by AFM to the self-assembly of the liquid-crystalline molecules.

AFM images of as-cast film of **2** are shown in Fig. 6. Both height (Fig. 6a) and phase (Fig. 6b) images clearly show the formation of the fiber-like nanostructures. Thermal annealing at 50 °C for 5 minutes under N_2 enhanced the structural order. A high resolution AFM phase image (Fig. 7) revealed long, partially aligned fibers with a width of around 10 nm and a length as long as 200 nm. As for the width, however, the broadening effect of the AFM tip should be taken into account, since the width of the fiber is comparable to the curvature radius of the tip (2 nm).[22] The corrected fiber width was calculated to be around 7 nm. XRD of the bulk **2** in powder form was also investigated at 20 °C (Fig. 8). The XRD pattern shows a peak at 50.2 Å and the secondary order diffraction peak at 25.1 Å, which is quite similar to the XRD pattern of the smectic A phase of the oligothiophene **1** shown in Fig. 4. This result suggests that the layered structure of the oligothiophene groups can be formed in the same manner even when the bulky fullerene groups are attached. The similarity of the fiber-like nanostructures in the dyad film to those in the oligothiophene film also suggests supramolecular self-assembly

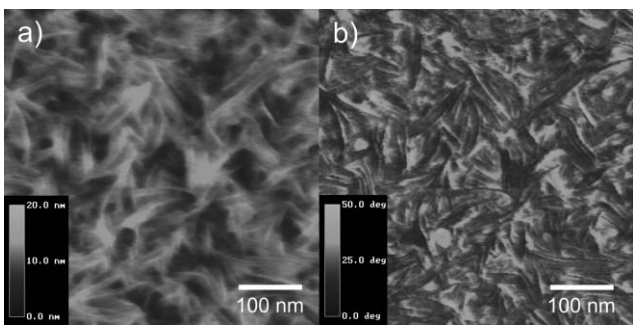

Fig. 6 AFM a) height and b) phase images of the dyad **2** film on ITO/PEDOT–PSS substrate.

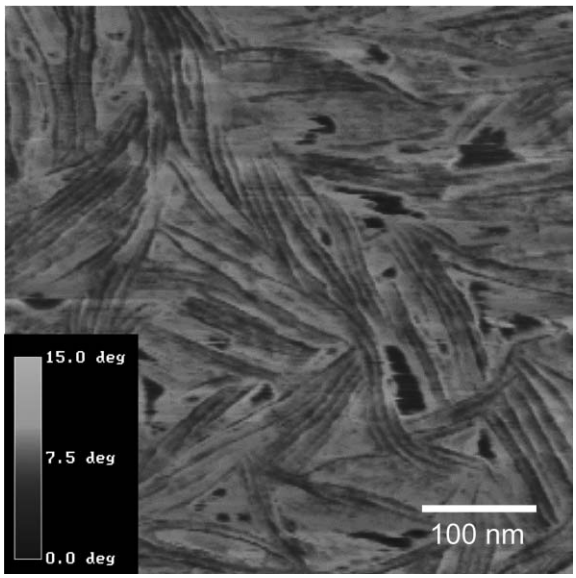

Fig. 7 AFM phase images of the dyad **2** film annealed at 50 °C for 5 min, observed with a super-sharp silicon probe.

of the molecule driven by π–π interaction of the oligothiophene groups. Considering the covalent attachment of both the oligothiophene and the fullerene groups, the formation of the fiber-like nanostructure in the dyad **2** film also implies spontaneous anisotropic organization of the fullerene group in the ordered structures. A possible molecular alignment is schematically shown in the inset of Fig. 8.

Optical properties

Optical absorption spectra of the thin films of the oligothiophene **1** and the dyad **2** on quartz/PEDOT–PSS substrates are shown in Fig. 9. The thin films were fabricated in the same manner as the films for AFM measurement except quartz substrates were used instead of ITO substrates. A film of a 1 : 1 molar ratio mixture of **1** and [6,6]-phenyl-C_{61}-butyric acid methyl ester (PCBM **3** in Fig. 1) was also investigated as a control. Both the films of **1** and the **1/3** mixture show π–π* absorption of the oligothiophene chromophore around 420 nm, which is blue-shifted compared to those in $CHCl_3$ solution

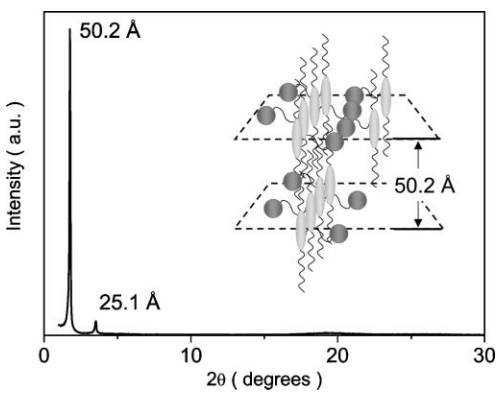

Fig. 8 The powder XRD pattern of the dyad **2** in the bulk measured at 20 °C. Inset: schematic representation of the proposed structure for the dyad molecules in the films.

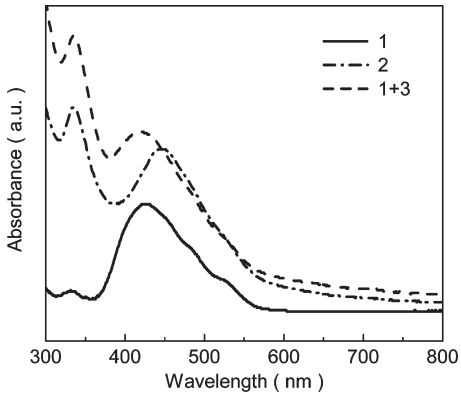

Fig. 9 Absorption spectra of the thin films of **1** (solid line), **2** (dashed-dotted line), and the mixture of **1** and **3** (dashed line).

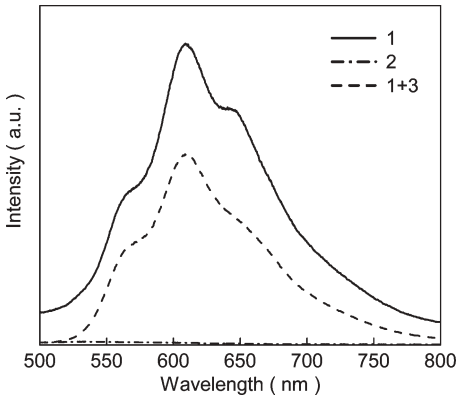

Fig. 11 Fluorescence spectra of the thin films of **1** (solid line), **2** (dashed-dotted line), and the mixture of **1** and **3** (dashed line).

(440 nm, not shown). This could be attributed to the formation of H-aggregation of the oligothiophene groups in those films. This also implies that the oligothiophene and PCBM exist separately in the mixture films. Indeed, the AFM image of the **1/3** mixture film in Fig. 10 shows two different regions of domains with fiber-like features and featureless domains of around 100-200 nm in size, indicating the phase separation of **1** and **3** in the film. In contrast, the dyad **2** film shows an absorption peak around 447 nm, which is slightly red-shifted compared to that in $CHCl_3$ solution. This result suggests that strong interaction and bulky characteristics of the fullerene groups change the aggregation manner of the oligothiophene groups in the dyad **2** film, possibly into a J-aggregation type.

To investigate the photo-induced electron transfer process in the films of the oligothiophene **1**, the mixture of **1/3** and the dyad **2**, fluorescence spectra were observed (Fig. 11). The dyad **2** film showed almost complete quenching of the fluorescence from the oligothiophene chromophore at around 610 nm when excited at 430 nm. In contrast, partial quenching was observed with the film of the **1/3** mixture. These results suggest that the electron transfer from the oligothiophene to the fullerene takes place more efficiently in the dyad **2** film than in the **1/3** mixture film. This enhancement could be explained mainly by the enlargement of the D–A interface in the dyad **2** film suggested by the AFM images (Fig. 6 and Fig. 10).

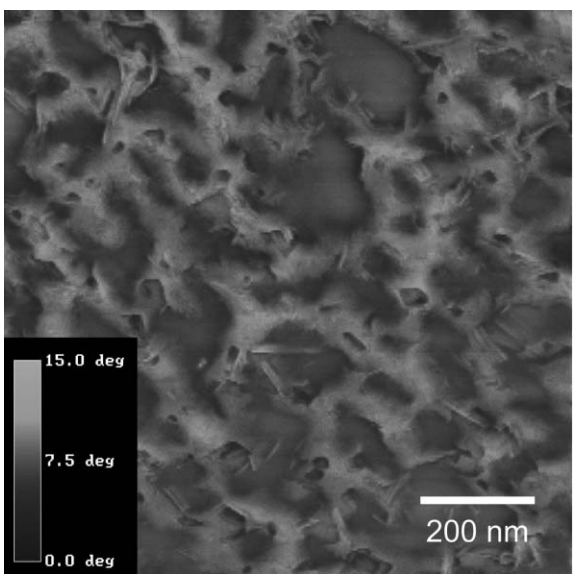

Fig. 10 AFM phase image of the thin film of the mixture **1** and **3** on ITO/PEDOT–PSS substrate.

Photovoltaic devices

Photovoltaic devices were fabricated with the configuration of ITO/PEDOT–PSS/**2**/Al. For comparison, a photovoltaic device of the mixture of **1** and **3** (1 : 1 molar ratio) was also fabricated in the same manner. Fig. 12 shows the I–V characteristics of the devices. Under simulated solar light (AM 1.5, 100 mW cm^{-2}) the dyad device showed I_{SC} = 0.93 mA cm^{-2}, V_{OC} = 0.70 V, FF = 0.23, resulting in a higher power conversion efficiency (PCE) of 0.15% compared to that of the mixture device (PCE = 0.09%, I_{SC} = 0.53 mA cm^{-2}, V_{OC} = 0.61 V, and FF = 0.28). As expected from the fluorescence quenching measurement in the films, the photocurrent was increased in the dyad **2** device. However, the relatively poor FF of the device limits the power conversion efficiency. This might be attributed to inefficient charge transport in the films because of unsuitable molecular packing of the oligothiophene and/or the fullerene groups or low alignment of their domains in the films. Fig. 13 shows the external quantum efficiencies (EQE) of the devices under

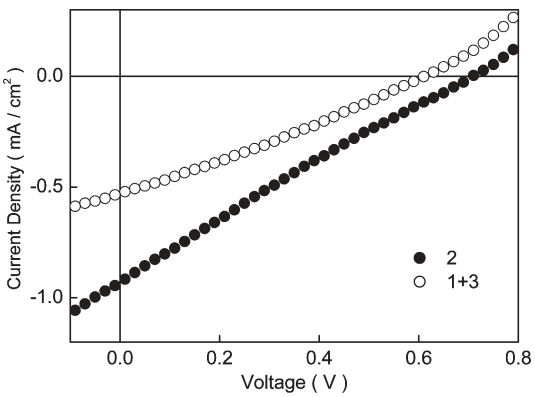

Fig. 12 I–V Characteristics of the photovoltaic devices of **2** (closed) and the mixture of **1** and **3** (open).

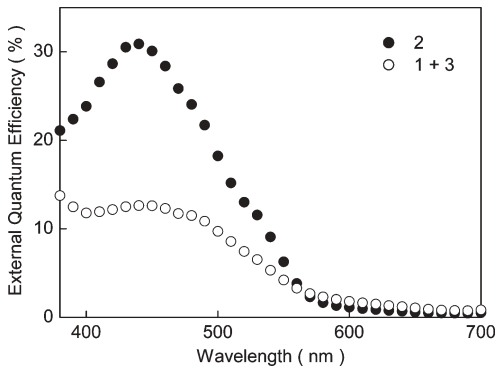

Fig. 13 External quantum efficiencies of the photovoltaic devices with **2** (closed) and the mixture of **1** and **3** (open).

monochromatic light irradiation. The dyad **2** device resulted in an improved EQE of 31% (440 nm), compared to EQE of 12% (420 nm) for the mixture device. The observed EQE is, to our knowledge, the highest value reported so far for dyad-based photovoltaic devices.[23–27] The improved quantum efficiency could be attributed to the large interface of the small domains of the oligothiophene and the fullerene groups formed in the dyad film, leading to enhanced charge separation. Furthermore, it is possible that the fibrous aggregation of the dyad molecules observed by AFM could facilitate intermolecular hopping of the separated charges and thus suppress charge recombination.

Conclusions

In conclusion, we have synthesized a novel liquid-crystalline oligothiophene and an oligothiophene-fullerene dyad to form supramolecular nanostructures in the solid film. Our preliminary result on the application for photovoltaic devices suggested that optimization of the molecular structure and alignment of this supramolecular structure could provide us a strategy to achieve high performance opto-electronic devices through spontaneous formation of nanostructures.

Experimental

Materials and instruments

1-(2*H*-Tetrahydropyran-2-yloxy)-17-{2,5-bis(trimethylstannyl) thiophene-3-ethoxy}-3,6,9,12,15-pentaoxaheptadecane **4**, 5-bromo-5″-hexadecyloxymethyl-2,2′–5′,2″-terthiophene **5**, 1-(3-carboxypropyl)-1-phenyl[6,6]C_{61} were synthesized using methods based on the literature procedures. Tetrakis(triphenylphosphine) palladium(0) was purchased from Tokyo Kasei Kogyo. Pyridinium *p*-toluenesulfonate, thienyl chloride, sodium hydride, and all organic solvents were purchased from Wako Chemicals. All of the chemicals were used as received unless otherwise mentioned.

Atomic force microscopy(AFM) images were obtained by Digital Instrumental Nanoscope31 operated in the tapping mode. The XRD pattern of the liquid-crystalline phase of **1** was measured using a Rint TTRII at Rigaku Corporation with Cu Kα operated at 50 kV voltage and 300 mA current. The XRD pattern of dyad **2** was measured using a Rigaku RCD-Rint 2400H with Cu Kα operated at 40 kV voltage and 100 mA current. Absorption spectra were measured using a SHIMADZU spectrophotometer MPC-3100. Fluorescence spectra were measured using a HITACHI F-4500 fluorescence spectrophotometer.

Compound 6

5-Bromo-5″-hexadecyloxymethyl-2,2′–5′,2″-terthiophene **5** (4.0 g, 6.9 mmol), 1-(2*H*-tetrahydropyran-2-yloxy)-17-{2,5-bis-(trimethylstannyl)thiophene-3-ethoxy}-3,6,9,12,15-pentaoxaheptadecane **4** (2.8 g, 3.5 mmol), and tetrakis(triphenylphosphine) palladium(0) (1 g, 0.87 mmol) were dissolved in 100 ml of dry toluene. The solution was treated by bubbling with N_2 for 5 min, and then heated to reflux for 22 h. The solution was filtrated to remove Pd catalysts and evaporated. The crude product was purified by silica-column chromatography eluting with ethyl acetate–hexanes (4 : 1), yielding 1.1 g (21%) of compound **6**. ^{1}H NMR (400 MHz, $CDCl_3$), δ (ppm): 7.12–7.03 (m, 11H), 6.85 (d, J = 3.6 Hz, 2H), 4.63 (s, 5H), 3.88–3.83 (m, 2H), 3.78–3.47 (m, 26H), 3.50 (t, J = 6.8 Hz, 4H), 3.08 (t, J = 6.8 Hz, 2H), 1.90–1.50 (m, 6H), 1.63–1.55 (m, 4H), 1.45–1.10 (m, 56H), 0.88 (t, J = 6.8, 6H). MALDI TOF-MS *m*/*z*: 1478.28 (calc.), 1476.77 (found, M^+).

Oligothiophene 1

Compound **6** (1.1 g, 0.73 mmol) and pyridinium *p*-toluenesulfonate (0.24 g, 0.96 mmol) were dissolved in 70 ml of $CHCl_3$–EtOH (1 : 1), and the solution was heated at 60 °C for 19 h. The solution was evaporated, and the crude product was purified by silica-column chromatography eluting with $CHCl_3$–ethyl acetate–methanol (50 : 30 : 1), yielding 0.52 g (51%) of oligothiophene **1**. ^{1}H NMR (500 MHz, $CDCl_3$), δ (ppm): 7.13–7.02 (m, 11H), 6.89 (d, J = 3.0 Hz, 2H), 4.63 (s, 4H), 3.78–3.58 (m, 26H), 3.50 (t, J = 6.4 Hz, 4H), 3.08 (t, J = 7.0 Hz, 2H), 1.61 (p, J = 7.0 Hz, 4H), 1.39–1.21 (m, 52H), 0.88 (t, 7.0 Hz, 6H). MALDI TOF-MS *m*/*z*: 1392.64 (calc.), 1392.1 (found).

Dyad 2

According to the report of Hummelen *et al.*,[28] a fullerene derivative with carboxylic chloride **7** was synthesized, prior to the esterification with **1**.

Thienyl chloride (0.98 g, 8.2 mmol) was added to a solution of 1-(3-carboxypropyl)-1-phenyl[6,6]C_{61} (80 mg, 0.089 mmol) in 20 ml of freshly distilled CS_2, and the solution was heated to reflux for 21 h. After all the volatile components were removed *in vacuo*, sodium hydride (5 mg, 0.22 mmol), toluene (10 ml), and **1** (62 mg, 0.045 mmol) dissolved in 10 ml of toluene were added to the residue (compound **7**). The mixed solution was stirred for 3 days, and then the solution was evaporated. The product was purified by silica-column chromatography eluting with ethyl acetate–hexanes (4 : 1), yielding 41 mg (40%) of dyad **2**. ^{1}H NMR (500 MHz, $CDCl_3$), δ (ppm): 7.90 (d, J = 7.5 Hz, 2H), 7.53 (t, J = 7.5 Hz, 2H), 7.49–7.42 (m, 1H), 7.13–7.02 (m, 11H), 6.89 (d, J = 3.0 Hz, 2H), 4.63 (s, 4H), 4.22 (t, J = 4.7 Hz, 2H), 3.77–3.60 (m, 24H), 3.50 (t, J = 6.6 Hz, 4H), 3.07 (t, J = 6.8 Hz, 2H), 2.91–2.86 (m, 2H), 2.53 (t,

J = 7.5 Hz, 2H), 2.20–2.14 (m, 2H), 1.61 (p, J = 6.9 Hz, 4H), 1.38–1.23 (m, 52H), 0.88 (t, J = 6.6 Hz, 6H). MALDI TOF-MS m/z: 2270.71 (calc.), 2270.4 (found).

Photovoltaic device preparation and measurement

Photovoltaic devices were prepared with the dyad **2** and the mixture of oligothiophene **1**/PCBM **3** in a structure of ITO/PEDOT–PSS/**2** (or **1**/**3**)/Al. ITO-coated glass substrates (R_s = 10 Ω per square, Kuramoto Japan) were cleaned by ultra-sonication in detergent, water, acetone, and 2-propanol. After drying the substrate, PEDOT–PSS (Baytron P) was spin-coated (4000 rpm) on ITO. The film was dried at 140 °C under N_2 for 10 min. After cooling the substrate, $CHCl_3$ solution of the dyad **2** (16 mg ml^{-1}) was spin-coated (2000 rpm). The film was dried with a N_2 flow for 30 min. For the mixture device, the solution was prepared by dissolving 16 mg of the oligothiophene **1** and 1 equivalent (10.5 mg) of PCBM **3** in 1 ml of $CHCl_3$, and the film was fabricated in the same manner. Finally, the Al electrode was evaporated on the organic layer under high vacuum (6×10^{-4} Pa). A HAYASHI LA-210UV xeon lamp and a USHIO SX-UID501CMQ xeon lamp with an AM 1.5 filter were used for EQE and PCE measurement, respectively. PCE of the devices were estimated at 100 mW cm^{-2}. The light intensity was adjusted with a silicon standard solar cell (Bunkou Keiki BS520).

Acknowledgements

We thank Dr K. Hirota for fruitful discussion, Mr Q. S. Wei for help with AFM measurement, and Rigaku Corporation for help with the XRD measurement.

References

1 F. J. M. Hoeben, P. Jonkheijm, E. W. Meijer and A. Schenning, *Chem. Rev.*, 2005, **105**, 1491–1546.
2 A. Schenning and E. W. Meijer, *Chem. Commun.*, 2005, 3245–3258.
3 F. S. Schoonbeek, J. H. van Esch, B. Wegewijs, D. B. A. Rep, M. P. de Haas, T. M. Klapwijk, R. M. Kellogg and B. L. Feringa, *Angew. Chem., Int. Ed.*, 1999, **38**, 1393–1397.
4 V. K. Praveen, S. J. George, R. Varghese, C. Vijayakumar and A. Ajayaghosh, *J. Am. Chem. Soc.*, 2006, **128**, 7542–7550.
5 X. Q. Li, V. Stepanenko, Z. J. Chen, P. Prins, L. D. A. Siebbeles and F. Wurthner, *Chem. Commun.*, 2006, 3871–3873.
6 J. van Herrikhuyzen, A. Syamakumari, A. Schenning and E. W. Meijer, *J. Am. Chem. Soc.*, 2004, **126**, 10021–10027.
7 A. M. Ramos, S. C. J. Meskers, E. H. A. Beckers, R. B. Prince, L. Brunsveld and R. A. J. Janssen, *J. Am. Chem. Soc.*, 2004, **126**, 9630–9644.
8 A. Ajayaghosh, R. Varghese, V. K. Praveen and S. Mahesh, *Angew. Chem., Int. Ed.*, 2006, **45**, 3261–3264.
9 S. J. George and A. Ajayaghosh, *Chem.–Eur. J.*, 2005, **11**, 3217–3227.
10 S. J. George, A. Ajayaghosh, P. Jonkheijm, A. Schenning and E. W. Meijer, *Angew. Chem., Int. Ed.*, 2004, **43**, 3422–3425.
11 O. Henze, W. J. Feast, F. Gardebien, P. Jonkheijm, R. Lazzaroni, P. Leclere, E. W. Meijer and A. Schenning, *J. Am. Chem. Soc.*, 2006, **128**, 5923–5929.
12 P. Leclere, M. Surin, P. Viville, R. Lazzaroni, A. F. M. Kilbinger, O. Henze, W. J. Feast, M. Cavallini, F. Biscarini, A. Schenning and E. W. Meijer, *Chem. Mater.*, 2004, **16**, 4452–4466.
13 P. Jonkheijm, N. Stutzmann, Z. J. Chen, D. M. de Leeuw, E. W. Meijer, A. Schenning and F. Wurthner, *J. Am. Chem. Soc.*, 2006, **128**, 9535–9540.
14 D. Hirayama, K. Takimiya, Y. Aso, T. Otsubo, T. Hasobe, H. Yamada, H. Imahori, S. Fukuzumi and Y. Sakata, *J. Am. Chem. Soc.*, 2002, **124**, 532–533.
15 H. Imahori and S. Fukuzumi, *Adv. Funct. Mater.*, 2004, **14**, 525–536.
16 E. E. Neuteboom, E. H. A. Beckers, S. C. J. Meskers, E. W. Meijer and R. A. J. Janssen, *Org. Biomol. Chem.*, 2003, **1**, 198–203.
17 C. C. You and F. Wurthner, *Org. Lett.*, 2004, **6**, 2401–2404.
18 G. X. Zhang, D. Q. Zhang, X. H. Zhao, X. C. Ai, J. P. Zhang and D. B. Zhu, *Chem.–Eur. J.*, 2006, **12**, 1067–1073.
19 F. Langa, M. J. Gomez-Escalonilla, J. M. Rueff, T. M. F. Duarte, J. F. Nierengarten, V. Palermo, P. Samori, Y. Rio, G. Accorsi and N. Armaroli, *Chem.–Eur. J.*, 2005, **11**, 4405–4415.
20 H. Zhang, F. J. M. Hoeben, M. J. Pouderoijen, A. Schenning, E. W. Meijer, F. C. Schryver and S. De Feyter, *Chem.–Eur. J.*, 2006, **12**, 9046–9055.
21 Y. Morikawa, S. Nagano, K. Watanabe, K. Kamata, T. Iyoda and T. Seki, *Adv. Mater.*, 2006, **18**, 883–+.
22 P. Samori, V. Francke, T. Mangel, K. Mullen and J. P. Rabe, *Opt. Mater.*, 1998, **9**, 390–393.
23 D. M. Guldi, C. P. Luo, A. Swartz, R. Gomez, J. L. Segura, N. Martin, C. Brabec and N. S. Sariciftci, *J. Org. Chem.*, 2002, **67**, 1141–1152.
24 N. Negishi, K. Takimiya, T. Otsubo, Y. Harima and Y. Aso, *Chem. Lett.*, 2004, **33**, 654–655.
25 F. S. Meng, J. L. Hua, K. C. Chen, H. Tian, L. Zuppiroli and F. Nuesch, *J. Mater. Chem.*, 2005, **15**, 979–986.
26 M. A. Loi, P. Denk, H. Hoppe, H. Neugebauer, C. Winder, D. Meissner, C. Brabec, N. S. Sariciftci, A. Gouloumis, P. Vazquez and T. Torres, *J. Mater. Chem.*, 2003, **13**, 700–704.
27 M. Narutaki, K. Takimiya, T. Otsubo, Y. Harima, H. Zhang, Y. Araki and O. Ito, *J. Org. Chem.*, 2006, **71**, 1761–1768.
28 J. C. Hummelen, B. W. Knight, F. LePeq, F. Wudl, J. Yao and C. L. Wilkins, *J. Org. Chem.*, 1995, **60**, 532–538.